Supplementary Materials for:

Enhancing energy storage performance via the artificial antiferroelectric strategy

Han Wu,[1,2] Kang-Ming Luo,[1,2] Mei-Xiong Zhu,[1,2] Yun-Long Tang,[1,2] Yin-Lian Zhu,[3,4,5] Xiu-Liang Ma,[3,4,6,7] and Yu-Jia Wang[1,2*]

[1] Shenyang National Laboratory for Materials Science, Institute of Metal Research, Chinese Academy of Sciences, 72 Wenhua Road, Shenyang, 110016, China.

[2] School of Materials Science and Engineering, University of Science and Technology of China, 72 Wenhua Road, Shenyang, 110016, China.

[3] Bay Area Center for Electron Microscopy, Songshan Lake Materials Laboratory, Dongguan 523808, Guangdong, China.

[4] Dongguan Institute of Materials Science and Technology, Chinese Academy of Sciences, Dongguan, 523808, China.

[5] School of Materials Science and Engineering, Hunan University of Science and Technology, Xiangtan 411201, China

[6] Institute of Physics, Chinese Academy of Sciences, Beijing 100190, China.

[7] Quantum Science Center of Guangdong-Hong Kong-Macau Greater Bay Area (Guangdong), Shenzhen 518000, China.

*E-mail: yjwang@imr.ac.cn

The supplementary materials contain:

Figs. S1 to S15

Supplementary Note 1: Free energy profiles and intrinsic coercive field from phenomenological theory

References

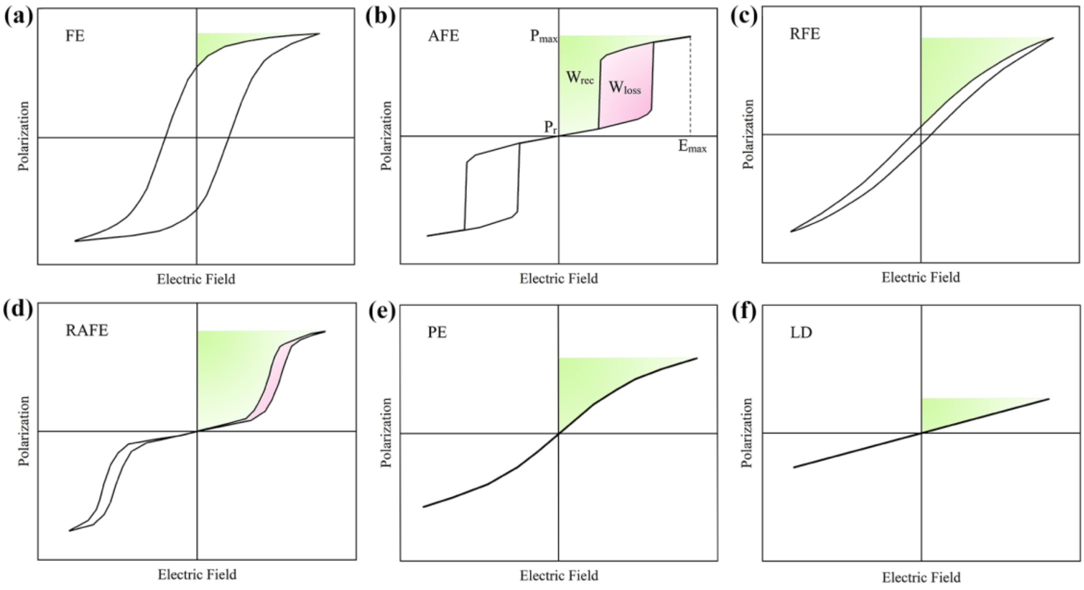

Fig. S1. Diagram of P-E hysteresis loops for (a) ferroelectrics (FE), (b) antiferroelectrics (AFE), (c) relaxor ferroelectrics (RFE), (d) relaxor antiferroelectrics (RAFE), (e) paraelectrics (PE), (f) linear dielectrics (LD) and some characteristic parameters for energy storage.

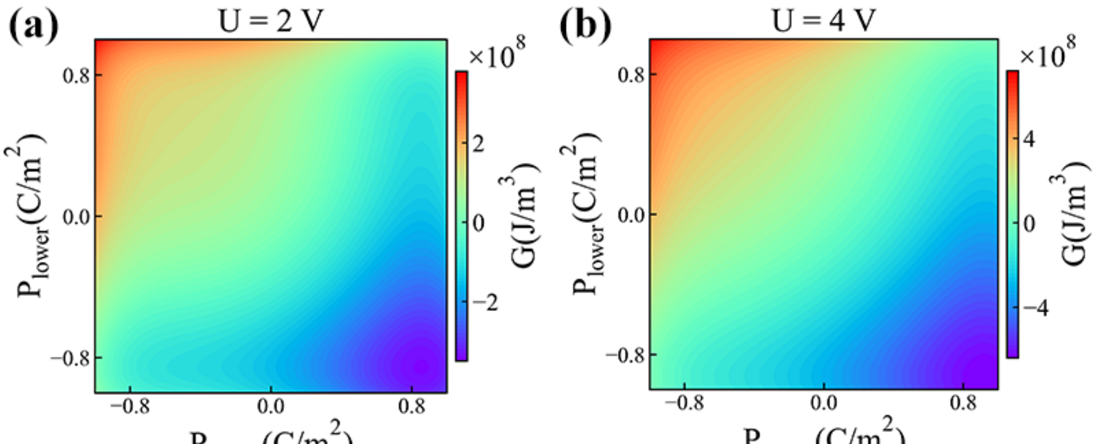

Fig. S2. The free energy landscape of the system as a function of P_{upper} and P_{lower} under $U = 2$ V (a) and 4 V (b).

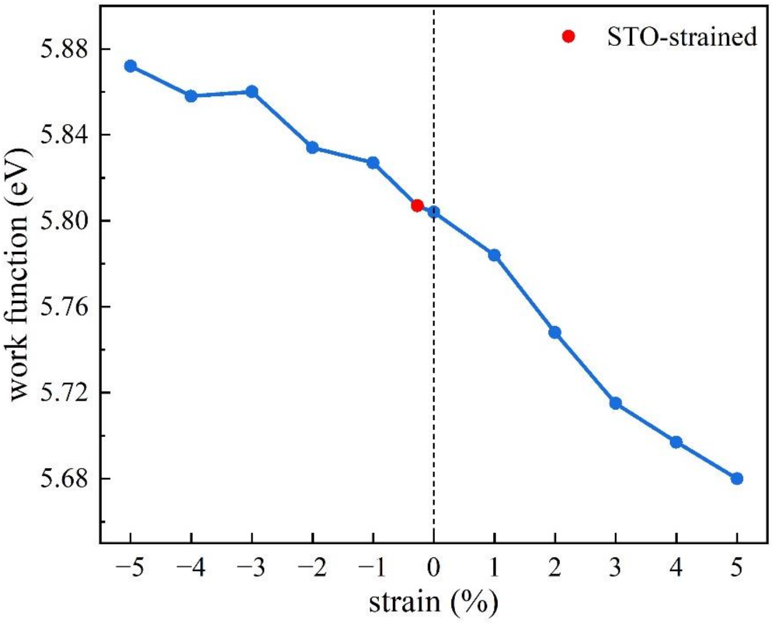

Fig. S3. The work function of the (001) surface of Pt at different strains.

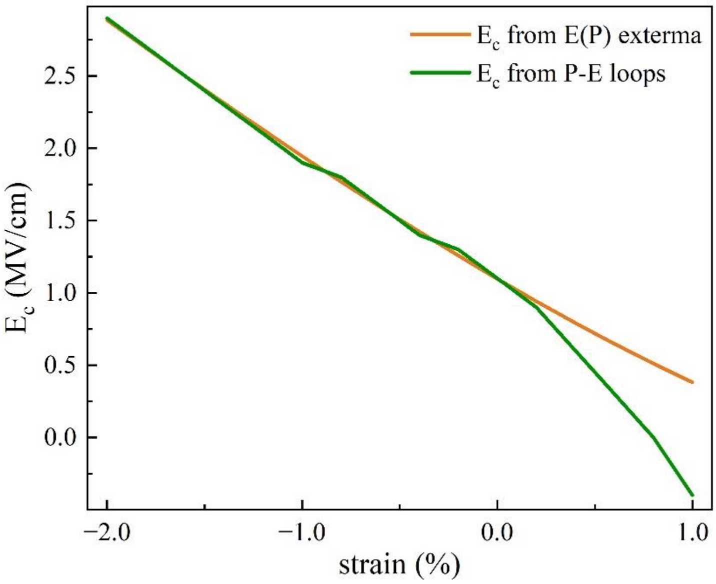

Fig. S4. Comparison between the coercive field extracted from the simulated P-E loops and the intrinsic coercive field obtained from the extrema of *E*(*P*).

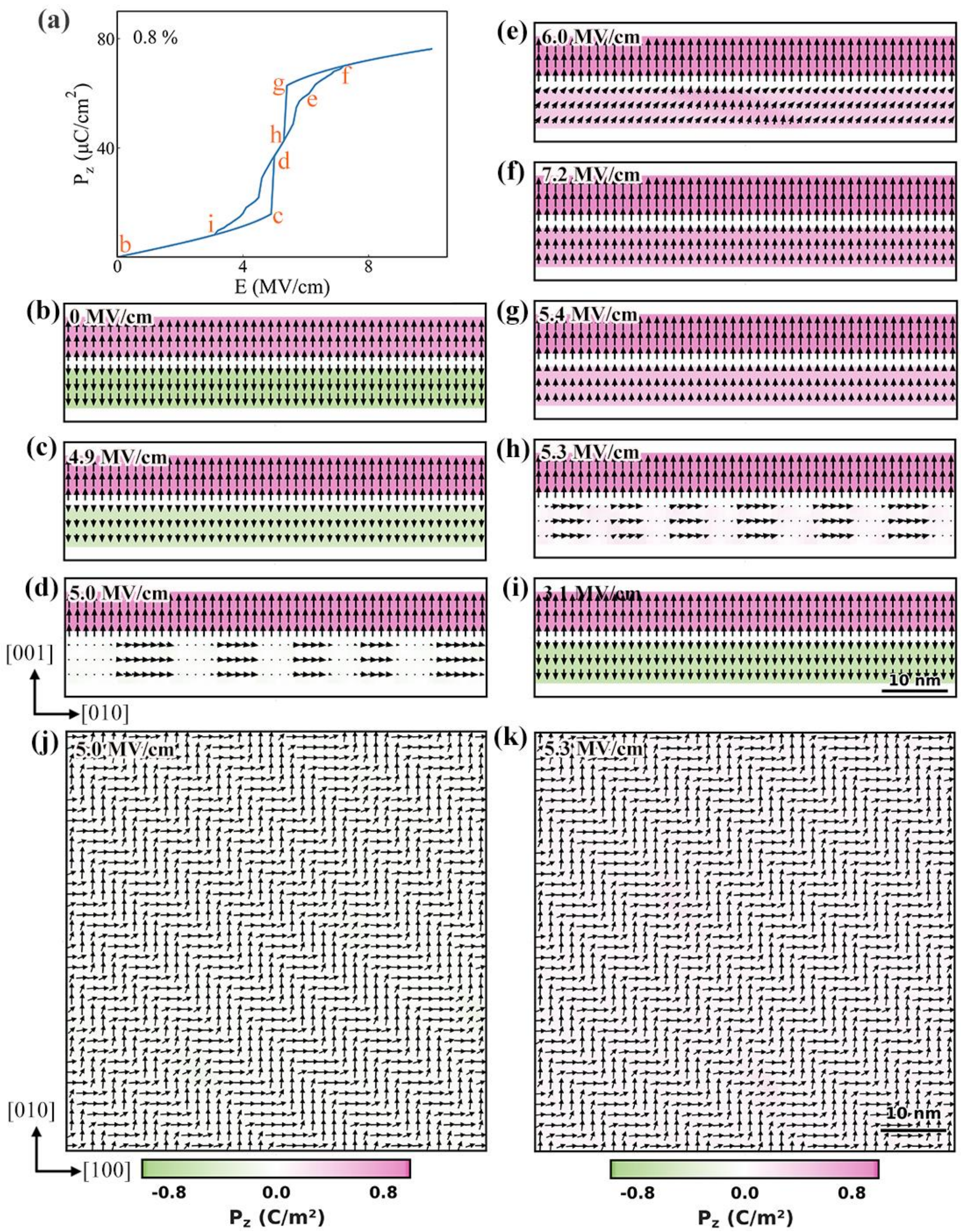

Fig. S5. The domain structure variation at the strain of 0.8% under U = 3 V. (a) The unipolar P-E hysteresis. (b)-(i) Polarization distributions of the model corresponding to points b-i on the hysteresis in a, respectively. (j), (k) The in-plane a_1/a_2 domain structure of the lower PTO film corresponding to points d and h on the hysteresis in a, respectively.

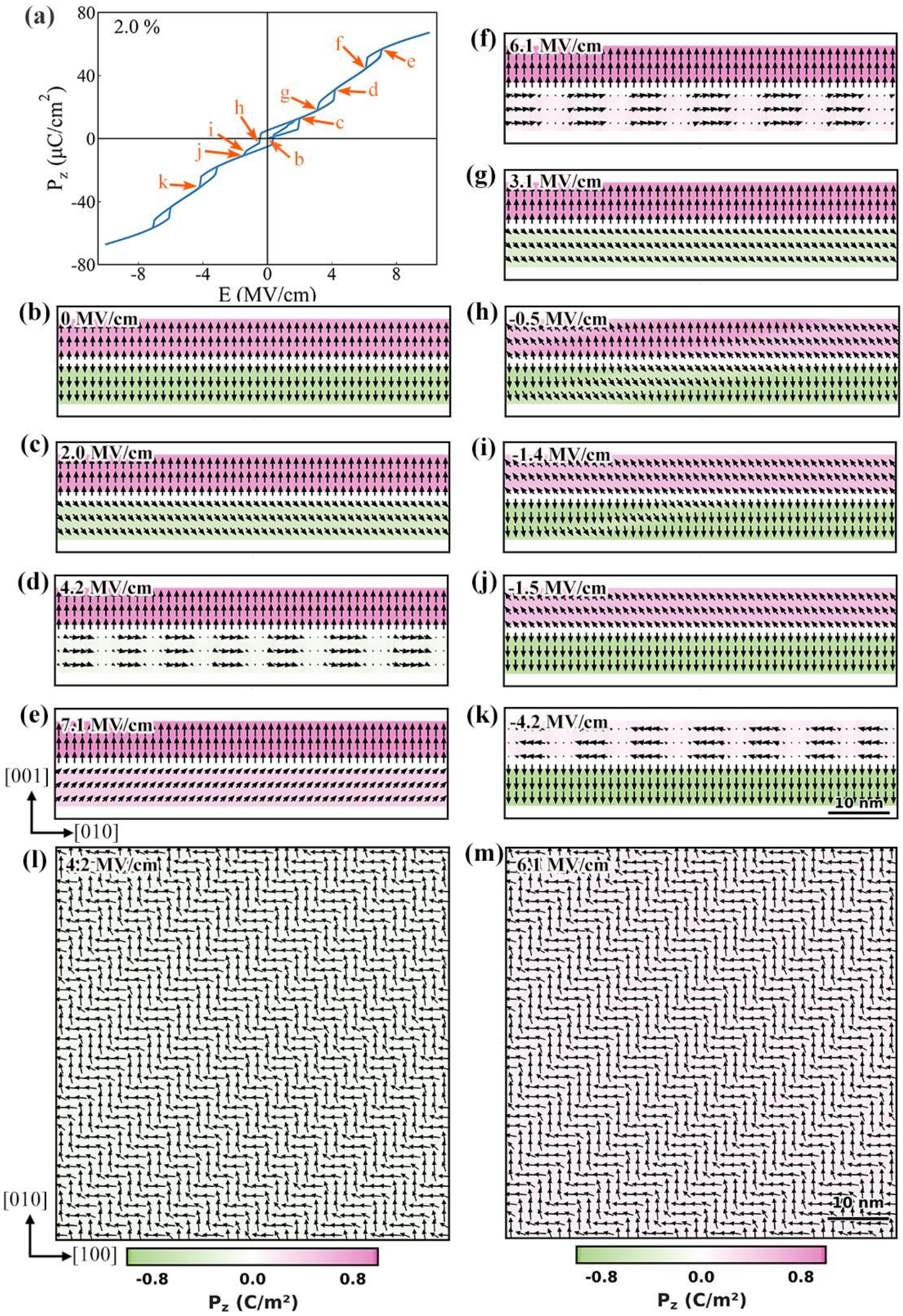

Fig. S6. The domain structures under different electric fields at the strain of 2.0% under $U = 3$ V. (a) The P-E hysteresis at a strain of 2.0%. (b)-(k) Polarization distributions of the model corresponding to points b-k on the hysteresis in a, respectively. (l), (m) The in-plane polarization distributions of the lower PTO film correspond to points d and f on the hysteresis in a, respectively.

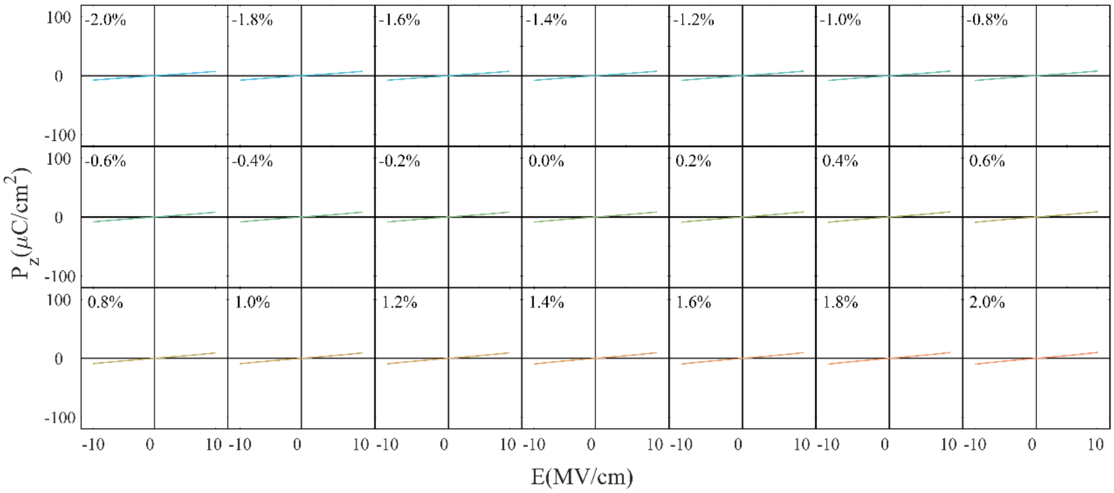

Fig. S7. P-E hysteresis at different strains at 2 nm

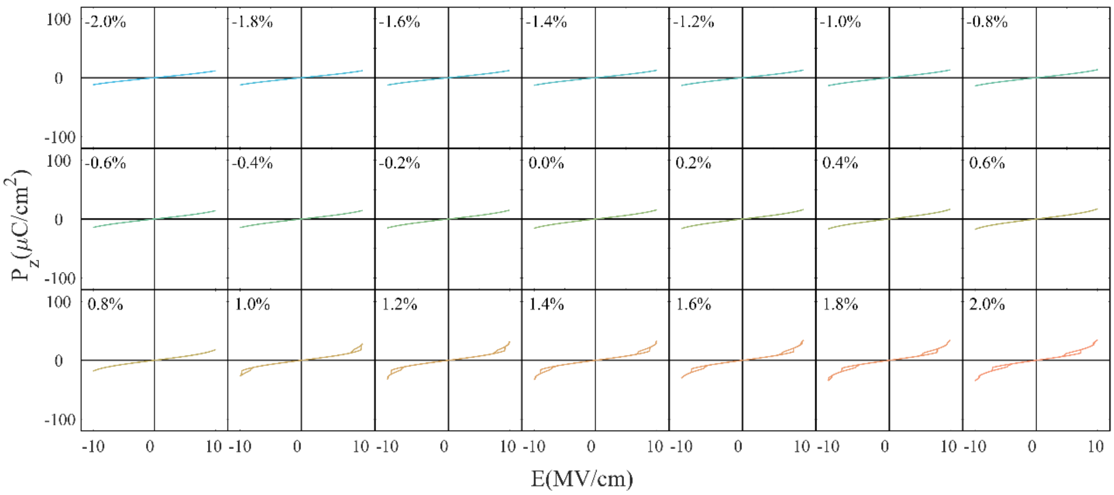

Fig. S8. P-E hysteresis at different strains at 3 nm

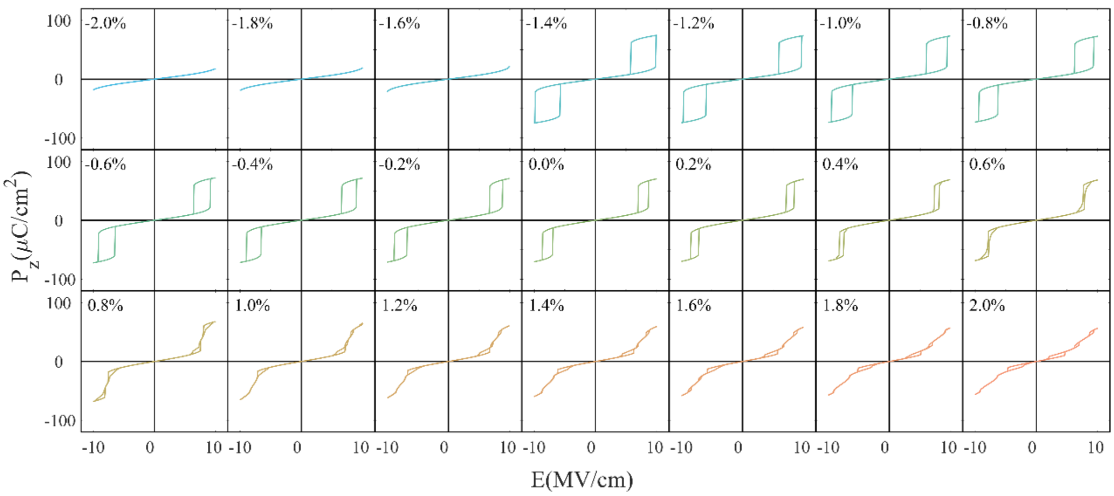

Fig. S9. P-E hysteresis at different strains at 4 nm

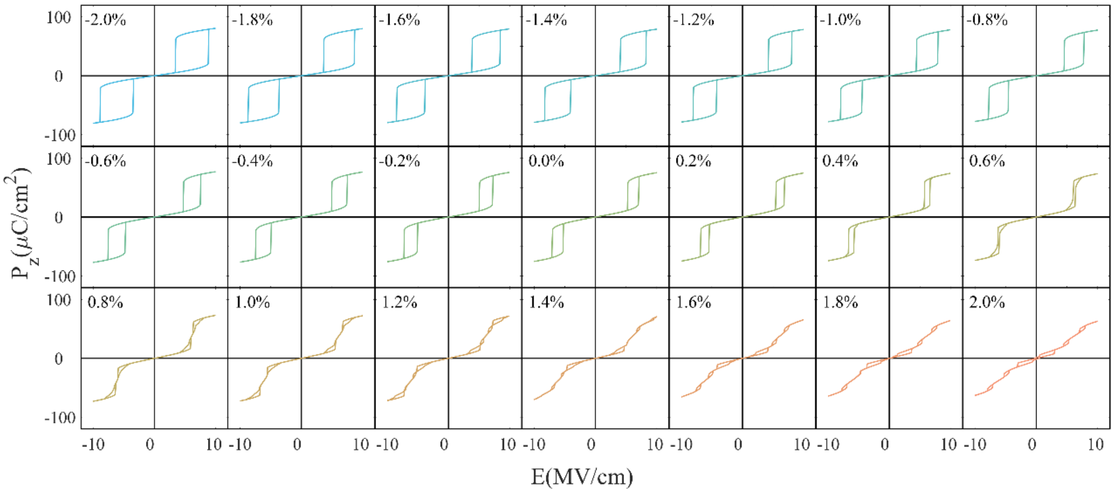

Fig. S10. P-E hysteresis at different strains at 5 nm

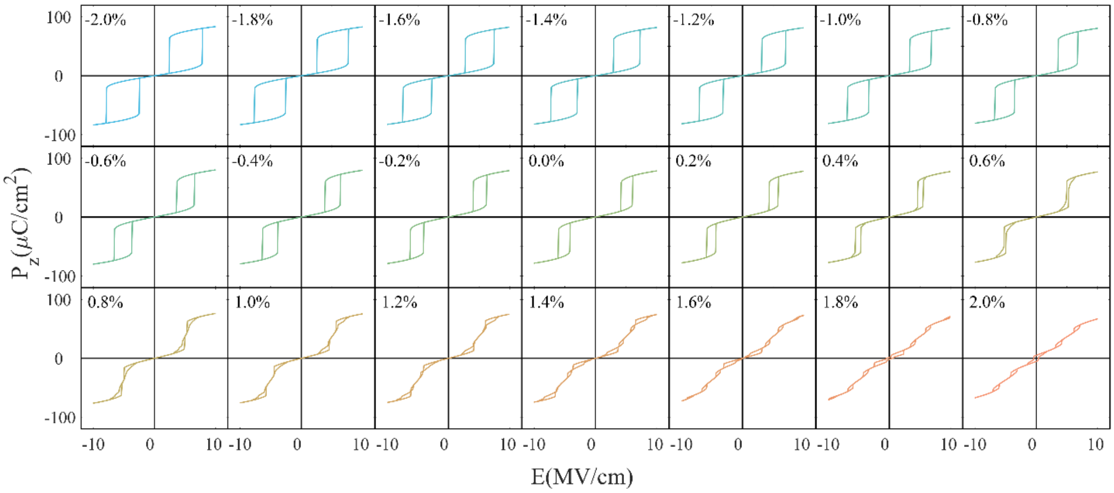

Fig. S11. P-E hysteresis at different strains at 6 nm

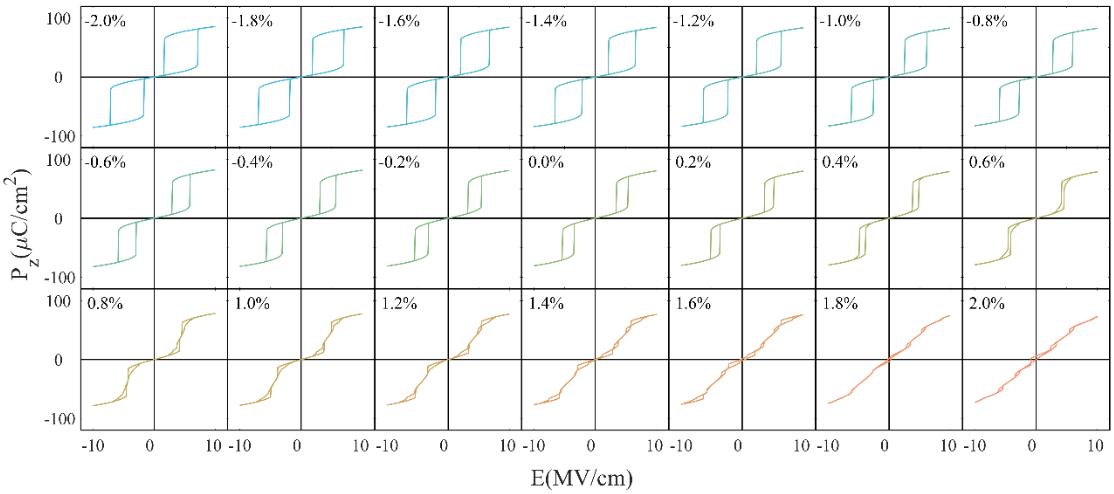

Fig. S12. P-E hysteresis at different strains at 7 nm

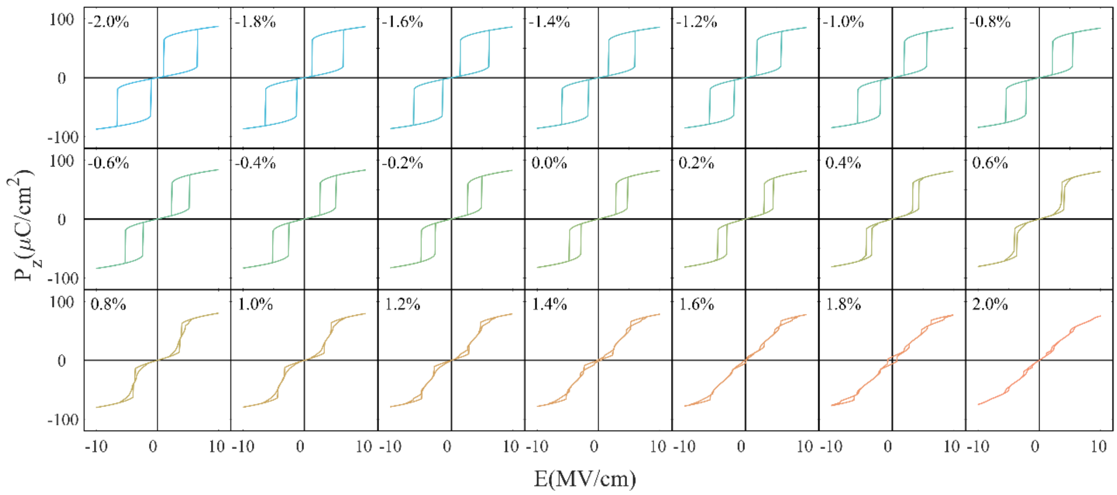

Fig. S13. P-E hysteresis at different strains at 8 nm

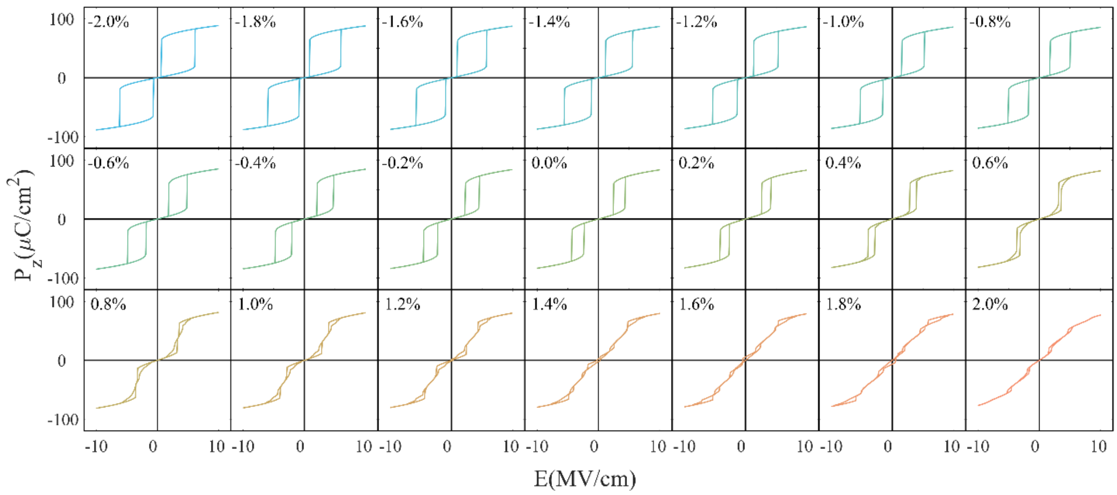

Fig. S14. P-E hysteresis at different strains at 9 nm

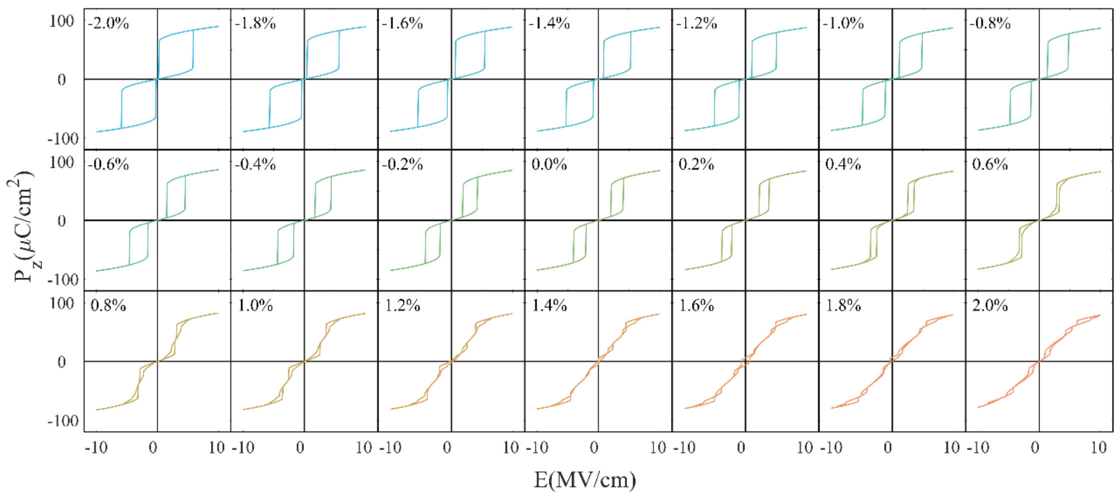

Fig. S15. P-E hysteresis at different strains at 10 nm

Supplementary Note 1: Free energy profiles and intrinsic coercive field from phenomenological theory

The thermodynamic treatment proposed by Pertsev et al., in which the misfit strain (μ_m) renormalizes the Landau coefficients through electrostrictive coupling[1] is employed to analyze the effect of strain on the coercive field. For an out-of-plane polarized *c*-domain, the free-energy density can be simplified as:

$$G = \alpha_3^* P_3^2 + \alpha_{33}^* P_3^4 + \alpha_{111} P_3^6 + \frac{\mu_m^2}{s_{11} + s_{12}} - EP_3 \quad (1)$$

where the renormalized coefficients are given by $\alpha_3^* = \alpha_1 - \mu_m \frac{2Q_{12}}{s_{11} + s_{12}}$, $\alpha_{33}^* = \alpha_{11} + \frac{Q_{12}^2}{s_{11} + s_{12}}$.

For the artificial antiferroelectric structure, the upper and lower ferroelectric layers experience opposite built-in electric fields ($E_{bi} = \frac{U}{h}$) induced by the work function difference. Therefore, the fields in the two layers are expressed as:

$$E_{upper} = E_{app} + E_{bi} \quad (2)$$

$$E_{lower} = E_{app} - E_{bi} \quad (3)$$

where E_{app} is the applied electric field.

The free energy densities of the upper (G_{upper}) and lower (G_{lower}) layers are calculated based on Eq. (1). Thus, the average free energy density of the system can be calculated by:

$$G = \frac{G_{upper} + G_{lower}}{2} \quad (4)$$

The stable states of the system can be obtained by selecting the minimum G with respect to variations of P_{upper} and P_{lower}.

The electric field is obtained from the first derivative of the free energy with respect to polarization,

$$E = 2\alpha_3^* P_3 + 4\alpha_{33}^* P_3^3 + 6\alpha_{111} P_3^5 \tag{5}$$

The intrinsic coercive field E_c is readily determined from the extrema of Eq. (5), i.e., from the turning point of the $E(P)$[2]. This analysis yields the relationship between the coercive field and the applied strain, as shown in Fig. S4. The results indicate that the intrinsic coercive field decreases monotonically with the decrease of compressive strain, which shows a good agreement with the coercive field from the simulated hysteresis loops in the strain range of -2.0 % ~ 0.2%. The coercive field from the P-E loops was derived from E_{A1} at $U = 3$ V for a PTO thickness of 6 nm, i.e., $E_C = E_{A1} - E_{bi}$, where $E_{bi} = \frac{U}{h}$. The difference between the coercive field extracted from the P-E loops and that predicted from the phenomenological theory under tensile strain arises because, at larger tensile strains, the polarization no longer reverses directly from the -*c* domain to the +*c* domain. The polarization with in-plane components appears during the switching process at larger tensile strain because of the tensile strain favors the formation of in-plane *a*-domains for a PTO film[3].

References

[1] N.A. Pertsev, A.G. Zembilgotov, A.K. Tagantsev, Effect of mechanical boundary conditions on phase diagrams of epitaxial ferroelectric thin films, Phys. Rev. Lett. 80 (1998) 1988–1991. https://doi.org/10.1103/PhysRevLett.80.1988.

[2] S. Ducharme, V.M. Fridkin, A.V. Bune, S.P. Palto, L.M. Blinov, N.N. Petukhova, S.G. Yudin, Intrinsic ferroelectric coercive field, Phys. Rev. Lett. 84 (2000) 175–178. https://doi.org/10.1103/PhysRevLett.84.175.

[3] A.R. Damodaran, S. Pandya, J.C. Agar, Y. Cao, R.K. Vasudevan, R. Xu, S. Saremi, Q. Li, J. Kim, M.R. McCarter, L.R. Dedon, T. Angsten, N. Balke, S. Jesse, M. Asta, S.V. Kalinin, L.W. Martin, Three-state ferroelastic switching and large electromechanical responses in PbTiO3 thin films, Adv. Mater. 29 (2017) 1702069. https://doi.org/10.1002/adma.201702069.